HOKKAIDO UNIVERSITY

Title	Effects of Crystal Size and Si/Al Ratio of MFI-type Zeolite Catalyst on n-Hexane Cracking for Light Olefin Synthesis
Author(s)	Konno, Hiroki; Okamura, Takuya; Nakasaka, Yuta et al.
Citation	Journal of the Japan Petroleum Institute, 55(4), 267-274 https://doi.org/10.1627/jpi.55.267
Issue Date	2012-07-01
Doc URL	https://hdl.handle.net/2115/50362
Type	journal article
File Information	JJPI55-4_267-274.pdf

Hokkaido University Collection of Scholarly and Academic Papers : HUSCAP

[Regular Paper]

Effects of Crystal Size and Si/Al Ratio of MFI-type Zeolite Catalyst on *n*-Hexane Cracking for Light Olefin Synthesis

Hiroki KONNO, Takuya OKAMURA, Yuta NAKASAKA, Teruoki TAGO*, and Takao MASUDA

Div. of Chemical System Engineering, Graduate School of Engineering, Hokkaido University, N13 W8, Kita-ku, Sapporo 060-8628, JAPAN

(Received February 2, 2012)

Catalytic cracking of *n*-hexane over MFI-type zeolite catalysts was examined at a reaction temperature of 823 K under atmospheric pressure. Conversion of *n*-hexane depended on the Si/Al ratio of the MFI-type zeolite catalyst, so the relationships between the product yields and *n*-hexane conversion could be fitted as single, smooth curves. To investigate the effect of crystal size of MFI-type zeolite on the catalytic activity, light olefin yield and product composition, nano- and macro-sized MFI-type zeolites with crystal sizes of approximately 150-200 nm and 1.5 μm, respectively, were prepared. The nano-sized zeolite exhibited a high *n*-hexane conversion with stable activity for 18 h compared with the macro-sized zeolite. The high activity of the nano-sized MFI-type zeolite is considered to be due to rapid diffusion of the produced light olefins out of the intracrystalline pores of the nano-zeolite due to the low diffusion resistance. Accordingly, the nano-sized zeolite achieved high yield of light olefins (approximately 35 %) and long catalyst lifetime.

Keywords

n-Hexane cracking, Light olefin, MFI zeolite catalyst, Nano zeolite catalyst, Low diffusion resistance

Introduction

Light olefins are important basic raw materials for the petrochemical industry, and demand for light olefins such as ethylene and propylene has been increasing every year[1),2)]. Light olefins have been mainly produced by thermal cracking of naphtha, which gives yields of ethylene and propylene of approximately 25 % and 13 %, respectively[3)~5)]. However, the naphtha cracking process consumes more than 30 % of the total amount of energy required in petrochemical production, so more efficient processes for the production of light olefins are highly desirable. Moreover, the relative demand for propylene has increased due to the large-scale production of ethylene in the Middle East and China. Catalytic cracking of naphtha over solid-acid catalysts can provide a high propylene/ethylene ratio at low reaction temperatures compared with thermal cracking[6)], so use of this process could provide energy savings together with the selective production of propylene. Accordingly, the catalytic cracking of naphtha is expected to be an effective alternative to the thermal cracking process.

Promising catalysts for *n*-hexane cracking include the zeolites, which are crystalline aluminosilicate materials with various properties, such as strong acidity and high surface area, and catalytic cracking of alkane over zeolite catalysts has been investigated[7)~9)]. Zeolites incorporate intracrystalline micropores and nanospaces close to the molecular diameters of light hydrocarbons, so have remarkable molecular-sieving effects for light hydrocarbons and have been widely used as shape-selective catalysts in various hydrocarbon processes, such as the alkylation of aromatics[10),11)] and synthesis of olefins from alcohol and acetone[12),13)]. However, the crystal sizes of zeolites are usually much larger than the sizes of the micropores, so the rate-limiting step of the reaction tends to be diffusion of the reactant/product molecules within the micropores. Moreover, carbon solid (coke) readily forms near the external surface of the crystal under diffusion-controlled conditions, resulting in rapid blocking of the pores, leading to a short catalyst lifetime. Nano-sized zeolites are effective to achieve low diffusion resistance, because the diffusion length for reactant/product hydrocarbons, which depends on the zeolite crystal size, is reduced.

We have successfully prepared MFI-type and MOR-type zeolite nanocrystals *via* hydrothermal synthesis in a water/surfactant/organic solvent (emulsion method)[14)~18)]. The nano-sized zeolites are expected to be effective catalysts with low diffusion resistance as well as large external surface area, which will improve the catalytic activity and lifetime. In the present study, catalytic cracking of *n*-hexane, as a model reaction for the catalytic cracking of naphtha, was examined over MFI-type zeolites, and the effects of the Si/Al ratio and

* To whom correspondence should be addressed.
* E-mail: tago@eng.hokudai.ac.jp

crystal size on the catalytic activity and stability were investigated. Catalytic cracking of naphtha is usually carried out above 873 K, where the catalytic and thermal cracking reactions simultaneously occur. To investigate the effects of the acidity and crystal size of zeolite on the cracking reaction in detail, the cracking reaction using the zeolite catalyst was examined at the reaction temperature of 823 K, where the thermal cracking is negligible.

1. Experimental

1. 1. Preparation of MFI-type Zeolite with Different Crystal Sizes

Nano-sized MFI-type zeolite was prepared *via* hydrothermal synthesis using a water/surfactant/organic solvent (emulsion method)[15]. An aqueous solution containing the Si and Al source material was obtained by hydrolyzing each metal alkoxide in a dilute tetrapropylammonium hydroxide (TPAOH)/water solution. The resultant water solution (10 mL) was added to a surfactant/organic solvent (70 mL, surfactant concentration of 0.5 mol/L). Polyoxyethylene-(15)-oleylether and cyclohexane were employed as the surfactant and organic solvent, respectively. The obtained water/surfactant/organic solvent was poured into a teflon-sealed stainless steel bottle and heated to 423 K for 72 h. To obtain macro-sized MFI-type zeolite, hydrothermal synthesis was also carried out without the surfactant/organic solvent (conventional method). The precipitates obtained were washed with alcohol, dried at 373 K for 12 h, and calcined at 823 K for 3 h in an air stream. Physically adsorbed and/or ion-exchanged sodium ions on the zeolite surface were removed and exchanged with NH_4^+ by a conventional ion exchange technique with 10 % NH_4NO_3 aqueous solution, and then heated to 823 K to yield a H-MFI-type zeolite. The resultant powdered zeolite was pelletized, crushed and sieved to yield samples *ca.* 0.3 mm in diameter for the synthesis of light olefins by *n*-hexane cracking.

The morphology and crystallinity of the obtained samples were analyzed using a field emission scanning electron microscope (FE-SEM; JSM-6500F, JEOL Ltd.) and an X-ray diffractometer (XRD; JDX-8020, JEOL Ltd.), respectively. The total and external surface areas of the obtained samples were calculated by the BET and the t-methods, respectively, using a N_2 adsorption isotherm device (Belsorp mini, BEL Japan Inc.). The Si/Al ratio of the obtained sample was measured by an X-ray fluorescence meter (XRF; supermini Rigaku Corp.). The chemical bonds of the aluminum atoms were characterized by ^{27}Al-NMR (Bruker MSL400). The acidity of the obtained samples was evaluated *via* the *ac*-NH_3-TPD method[19]. In the temperature-programmed desorption (TPD) experiment, the carrier gas was 1.0 % NH_3 (balance He), the heating rate was 5 K·min^{-1}, and the temperature range was 373 to 823 K. The desorption of NH_3 molecules from the acid sites of the zeolite was measured under a 1.0 % NH_3–He atmosphere so that the TPD profile could be measured under complete adsorption equilibrium conditions, here called the *ac*-NH_3-TPD method.

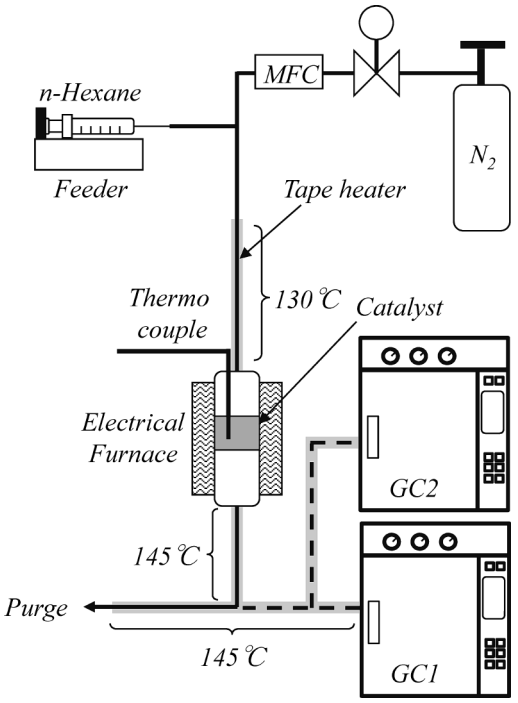

Fig. 1 Experimental Setup of the Fixed-bed Flow Reactor

1. 2. *n*-Hexane Cracking over Zeolite Catalysts

Cracking of *n*-hexane over zeolite catalysts was carried out using a fixed-bed reactor at a reaction temperature of 823 K under N_2 at atmospheric pressure. A schematic of the apparatus is shown in **Fig. 1**. *W*/*F* (*W*: amount of catalyst/g, *F*: feed rate/g·h^{-1}) was 0.5 h. The feed rate of *n*-hexane was 1.37×10^{-2} mol/h and catalyst weight was 0.589 g. The composition of the gaseous product was measured by on-line gas chromatography (GC-2014, Shimadzu Corp.) with a Porapak-Q column for the thermal conductivity detector (TCD) and Gaskuropack-54 and SP-1700 columns for the hydrogen-flame ionization detector (FID). The amount of coke deposited on the catalyst after reaction was measured by thermogravimetric analysis (TG; TGA-50, Shimadzu Corp.). The characteristics of the coke deposited on the catalyst (H/C ratio) were obtained by the elemental analysis (JM-10, J-Science Lab Co., Ltd.).

2. Results and Discussion

2. 1. Preparation of MFI-type Zeolites

To investigate the effect of the Si/Al ratio of MFI-type zeolites on the product selectivities and yields,

nano-sized zeolites with different Si/Al molar ratios (50, 80, 150, and 300) were prepared *via* hydrothermal synthesis in a water/surfactant/organic solvent[15]. **Figures 2** and **3** show the X-ray diffraction patterns and FE-SEM micrographs of the samples, respectively. The X-ray diffraction patterns of the samples with different Si/Al ratios showed peaks corresponding to MFI-type zeolite. Moreover, nano-sized zeolites with crystal sizes of approximately 150-200 nm were observed. Accordingly, nano-sized zeolites with different Si/Al ratios were obtained. The XRD pattern and FE-SEM micrograph of macro-sized zeolite are also shown for comparison, to illustrate macro-sized zeolite with crystal sizes of approximately 1.5 μm.

The positions and amount of Al atoms in the zeolite framework were evaluated by ^{27}Al-NMR measurement and XRF analysis, respectively. As shown in **Fig. 4**, the presence of a signal resonance centered at approximately 50-60 ppm is assigned to the tetrahedral Al atoms located in the internal framework of the zeolite. A signal resonance at 0 ppm is characteristic of the octahedral Al atoms located outside the framework of the zeolite. The ^{27}Al-NMR spectrum of these zeolites only indicated the presence of tetrahedral Al atoms, regardless of the crystal size and Si/Al ratio. Moreover, as listed in **Table 1**, the Si/Al values measured by XRF were almost the same for each Si/Al ratio calculated from Si and Al concentrations in the synthetic solution. Therefore, the Al atoms in the synthetic solution were incorporated into the framework structures of MFI-type zeolite during hydrothermal synthesis.

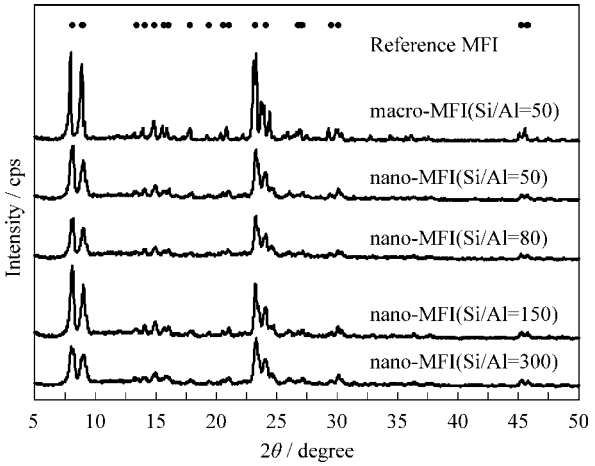

Fig. 2 XRD Patterns of Macro- and Nano-sized Zeolites

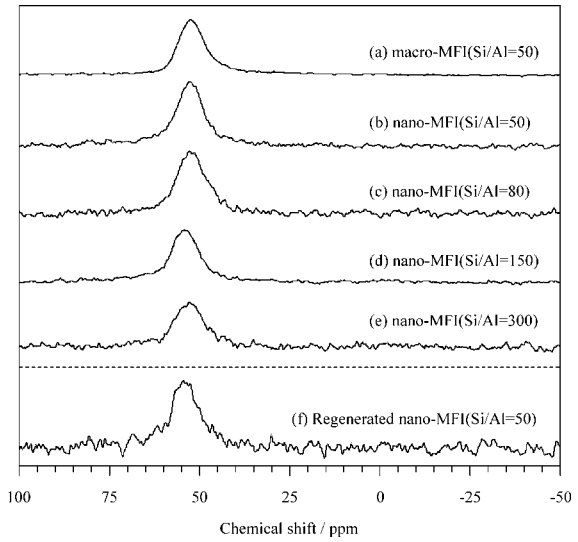

Fig. 4 ^{27}Al MAS NMR Spectra of Macro- and Nano-sized Zeolites before Reaction (a-e) and after Regeneration (f)

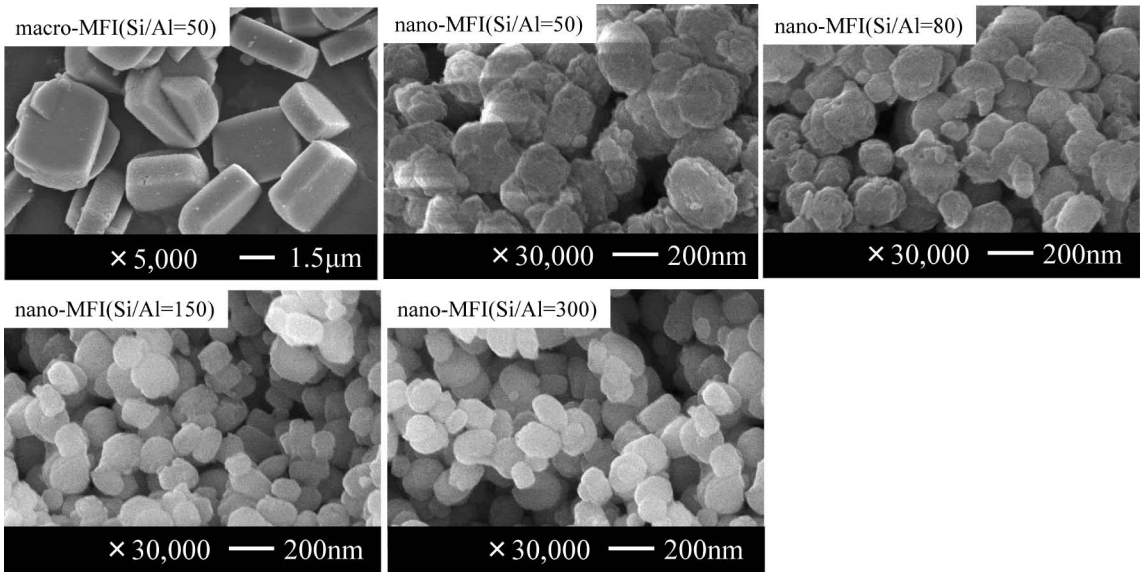

Fig. 3 SEM Micrographs of Macro- and Nano-sized Zeolites

Table 1 Calculated and Measured Si/Al Values, *n*-Hexane Conversion and Product Selectivities in *n*-Hexane Cracking over Nano-sized Zeolites

Catalyst	Si/Al ratio measured by XRF	*n*-Hexane conversion [C-mol%]	Selectivity [C-mol%]								
			CH_4	C_2H_4	C_2H_6	C_3H_6	C_3H_8	C_4H_8	C_4H_{10}	C_5	C_7^+	BTX
nanoMFI50	56.2	93.4	2.2	11.8	9.4	16.1	19.2	6.4	9.5	3.2	0.2	22.6
nanoMFI80	90.0	82.4	2.3	14.2	8.2	21.3	21.8	8.3	8.0	1.8	0.2	14.1
nanoMFI150	180.4	67.8	2.1	12.0	10.4	28.8	16.8	11.2	11.8	3.6	0.1	3.3
nanoMFI300	375.0	26.0	2.2	7.7	10.9	32.4	13.7	15.8	11.6	4.5	0.1	1.3

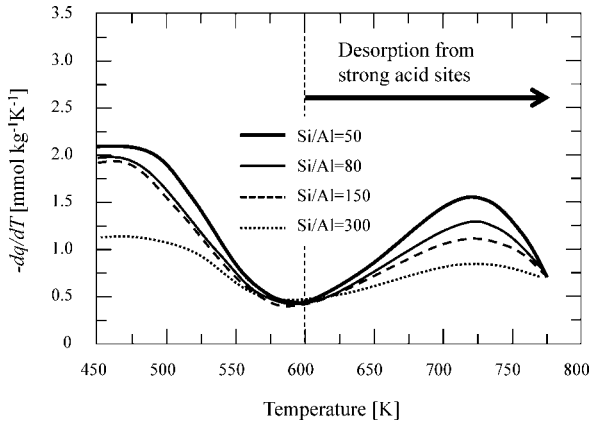

Fig. 5 NH_3-TPD Profiles of Nano-sized Zeolites with Different Si/Al Ratios

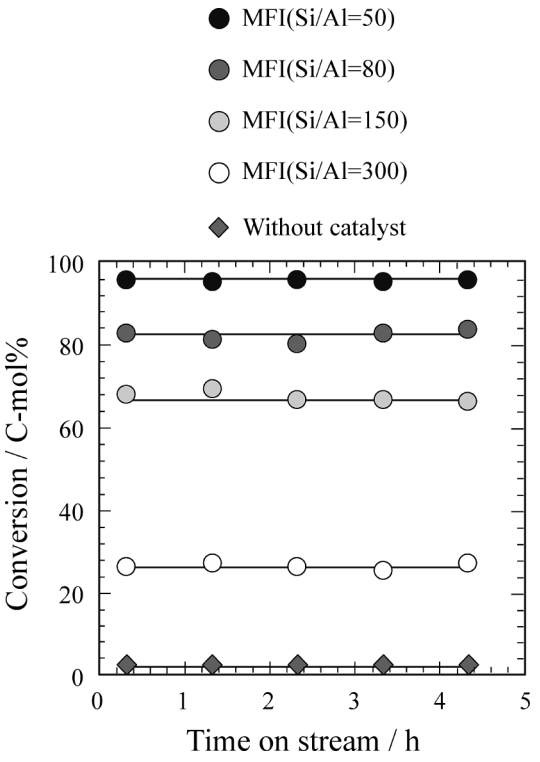

Fig. 6 *n*-Hexane Conversion with Reaction Time on Stream Using Nano-sized Zeolites with Different Si/Al Ratios

2. 2. Effect of Si/Al Molar Ratio of Nano-sized MFI-type Zeolite

Firstly, the effect of the Si/Al ratio on catalytic activity and product yields of *n*-hexane cracking was examined using nano-sized zeolites. **Figure 5** shows the NH_3-TPD profiles of the nano-sized zeolites with different Si/Al ratios. NH_3 desorption peaks were observed at temperatures above 600 K, which is associated with strong acid sites. Moreover, the area of the TPD profiles above 600 K depended on the Si/Al ratio of the zeolites. Accordingly, nano-sized zeolites with different acidities were obtained and could be used as catalysts for *n*-hexane cracking.

Figure 6 shows the changes in *n*-hexane conversion with time on stream over the nano-sized zeolites. The *n*-hexane conversion depended on the Si/Al ratio and increased with higher amounts of Al (lower Si/Al ratio), indicating that the reaction progressed over the acid sites of the zeolite. In thermal cracking without catalyst, the conversion of *n*-hexane was no more than 2.5 % under the experimental conditions, which was much lower than that obtained in catalytic cracking using the zeolite catalysts. Moreover, the conversion during catalytic cracking of *n*-hexane over the zeolites remained unchanged, and the nano-sized zeolite (Si/Al = 50) exhibited high conversion above 90 % with stable activity.

The product selectivities are listed in **Table 1** at an initial reaction time of 20 min. Products including alkanes (methane, ethane, propane, and butane), alkenes (ethylene, propylene, and butene) and aromatics (benzene, toluene, and xylene (BTX)) were obtained. In low *n*-hexane conversion (Si/Al = 300), the selectivities for propylene and butene were high (32.4 % and 15.8 %, respectively) because these products are formed *via* energetically favorable secondary or tertiary carbenium ions in the classical bimolecular mechanism)[20)~22)]. On the other hand, the selectivity of ethylene was low (7.7 %) because ethylene is formed *via* energetically unfavorable primary carbenium ions, regardless of the monomolecular or bimolecular mechanism)[20)~22)]. As the conversion increased (*i.e.*, decreasing Si/Al ratio), the selectivity for BTX increased whereas the selectivities for propylene and butene decreased, indicating that the products formed by cracking changed in accordance with the series of reactions. In contrast, the selectivities for methane and ethane were approximately 2 % and 10 %, respectively, and remained almost unchanged regardless of the *n*-hexane conversion. Methane and ethane are formed *via* a monomolecular mechanism[20)]. Therefore, both monomolecular and bimolecular crack-

ing occurred under the experimental conditions using the nano-sized zeolites.

To investigate the series of reactions in detail, the relationship between *n*-hexane conversion and the yields of light olefins and BTX was investigated, as shown in **Fig. 7**. The vertical axis of **Fig. 7** shows *n*-hexane conversion at the initial reaction time shown in **Fig. 6**. Conversion of *n*-hexane depended on the Si/Al ratio of the zeolite catalyst, so the relationships between the product yields and *n*-hexane conversion could be fitted as single, smooth curves. The yields of each light olefin increased with *n*-hexane conversion and reached maximum values, where the total yield of light olefins also reached a maximum value and slightly decreased with conversion. In contrast, the yields of BTX and paraffins monotonically increased with conversion, indicating that the light olefins were transformed into BTX. A maximum light olefin yield of approximately 35 C-mol% was obtained using nano-sized zeolite with a Si/Al ratio of 150, for which the aromatic yield was less than 3 C-mol%.

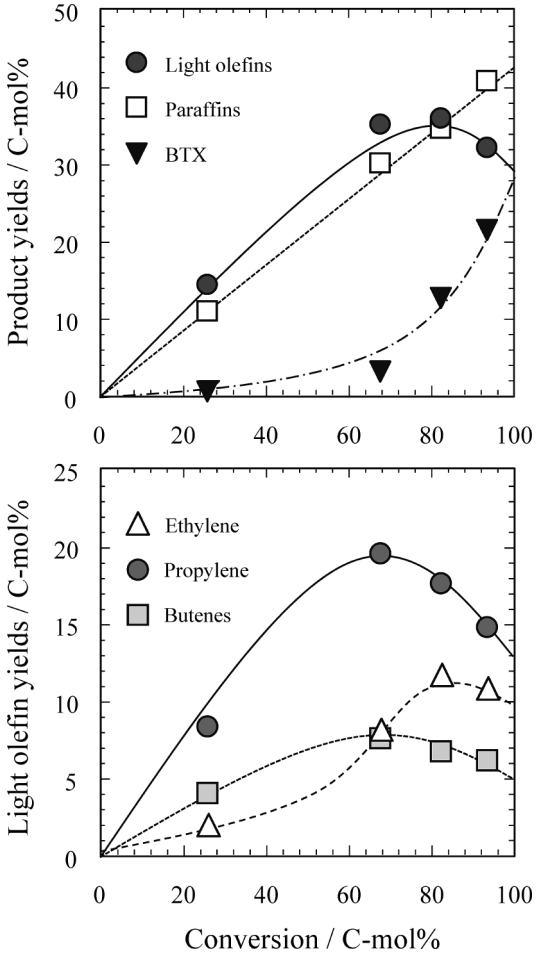

Fig. 7 Relationship between *n*-Hexane Conversion and Product Yields at Initial Reaction Time (20 min) over Nano-sized Zeolites with Different Si/Al Ratios

2. 3. Effect of Crystal Size of MFI-type Zeolite

In *n*-hexane cracking over MFI-type zeolites, propylene and butene were the primary products, followed by aromatics formed by a series of reactions, indicating that diffusion of the produced light olefins within the zeolite affected the product yields and catalyst lifetime. Accordingly, the effect of zeolite crystal size on the product selectivities and catalytic stability in *n*-hexane cracking was investigated using MFI-type zeolites with different crystal sizes shown in **Fig. 3**. The BET and external surface areas and Si/Al ratios of zeolites calculated from the N_2 adsorption isotherms and measured by XRF, respectively, are listed in **Table 2**. The NH_3-TPD profiles of macro- and nano-sized MFI-type zeolites are shown in **Fig. 8**. The BET surface areas of both zeolite samples were approximately 400 m^2/g, but the external surface areas varied depending on the crystal size. The Si/Al ratio of these zeolites measured by XRF were almost the same value of 50, so that these zeolites were expected to possess approximately the same acidity, which was confirmed by the NH_3-TPD profiles of these zeolites as shown in **Fig. 8**.

Changes in the *n*-hexane conversions and product yields over MFI-type zeolites (Si/Al = 50) with different crystal sizes are shown in **Fig. 9**. The product

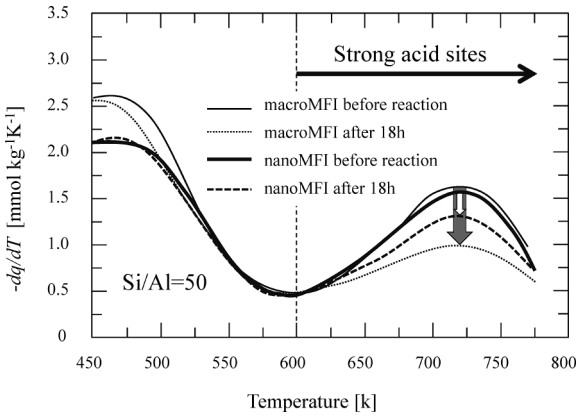

Fig. 8 NH_3-TPD Profiles of Macro- and Nano-sized Zeolites before and after Reaction for 18 h

Table 2 BET and External Surface Areas of Macro- and Nano-sized MFI-type Zeolites (Si/Al = 50)

Sample	S_{BET} [$m^2 \cdot g^{-1}$]	S_{ext} [$m^2 \cdot g^{-1}$]	Si/Al measured by XRF
macroMFI50	412.1	18.8	53.1
nanoMFI50	389.8	47.0	56.2

S_{BET}: surface area by BET method, S_{ext}: external surface area by t-method.

selectivities at the conversion of approximately 95 % (reaction times of 8.33 h and 4.33 h for nano- and macro-sized zeolites, respectively) are shown in **Fig. 10**; where the amount of methane, and alkanes comprising C_5 and C_7^+ are denoted as others. Although these MFI-type zeolites with different crystal sizes exhibited almost the same *n*-hexane conversion at the initial reaction time, the conversion gradually decreased with time on stream over the macro-sized MFI-type zeolite, falling to 85 % after 16 h. In contrast, a high conversion of 93 % was maintained after 16 h over the nano-sized MFI-type zeolite, hardly changing from the start of reaction. Additionally, the changes in light olefin and BTX yields with time on stream over the nano-sized zeolite were quite different from those over the macro-sized zeolite. As shown in **Figs. 9** and **10**, the total yield of light olefins over the nano-sized zeolite (32.4 %) was much higher than that over the macro-sized zeolite (23.2 %) at the *n*-hexane conversion of approximately 95 %, and this value was maintained for 18 h, whereas the BTX and olefin yields over the macro-sized zeolite monotonically changed with time on stream.

These findings revealed that the changes in conversion and product yields with time on stream depended on the crystal size of the catalyst. To investigate the effect of crystal sizes on deactivation in detail, the NH_3-TPD profiles after the reaction and the amount of coke deposited on these zeolites were measured. The NH_3-TPD profiles of these zeolites after the reaction are also shown in **Fig. 8**. Whereas the number of strong acid sites of nano-sized zeolite had slightly decreased after reaction at 18 h, that of macro-sized zeolite gradually decreased after reaction at 18 h. Moreover, the amounts and the H/C atomic ratio of the deposited coke on the zeolites were measured, as listed in **Table 3**. The amounts of coke formed on the nano- and macro-sized zeolites during cracking were 2.2 wt% and 7.3 wt%, respectively. Although the nano-sized zeolite

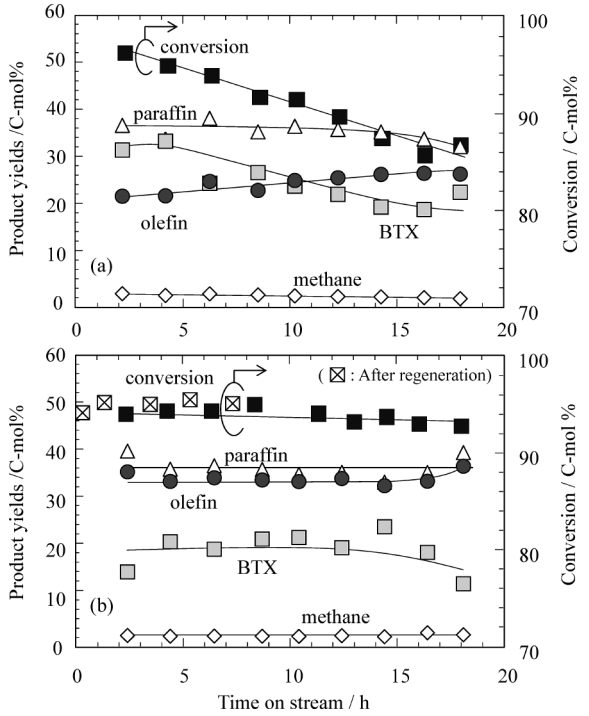

Conversion is also plotted using the nano-sized zeolite after regeneration treatment.

Fig. 9 Changes in *n*-Hexane Conversion and Product Yields with Time on Stream over (a) Macro- and (b) Nano-sized Zeolites (Si/Al = 50)

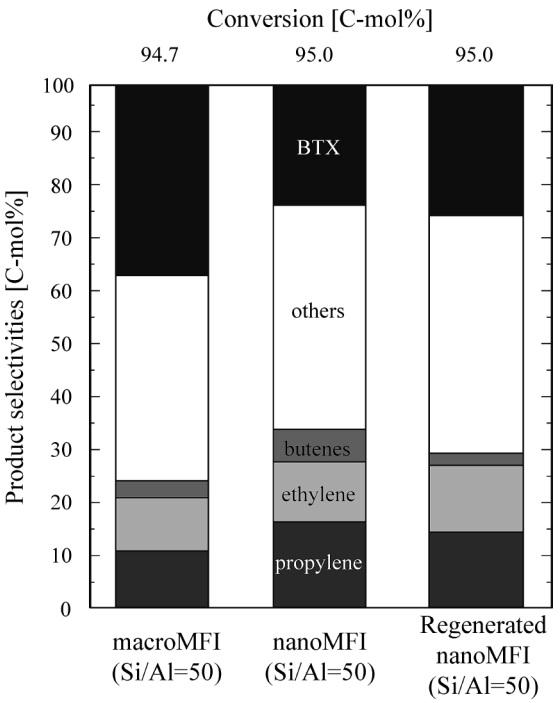

Selectivity is also shown using the nano-sized zeolite after regeneration treatment.

Fig. 10 Product Selectivities at *n*-Hexane Conversion of Approximately 95 C-mol% over Macro- and Nano-sized Zeolites (Si/Al = 50)

Table 3 Amount of Coke and the H/C Ratio of Deposited Coke on the Macro- and Nano-sized Zeolites (Si/Al = 50) after Reaction for 18 h

Sample	Coke amount [wt%]	H/C ratio measured by elemental analysis
macroMFI50	7.3	0.95
nanoMFI50	2.2	1.70

possessed a much larger external surface area than the macro-sized zeolite, the amount of coke formed on the nano-sized zeolite was approximately 3 times smaller than that formed on the macro-sized zeolite. Thermal cracking of *n*-hexane was negligibly small, as shown in **Fig. 6**, so the coke on the zeolites was derived from carbonaceous solids formed by catalytic cracking rather than thermal cracking. Since the diffusion resistance of the light olefin products increased with increasing crystal size, excessive reaction of the light olefins probably occurred in the macro-sized zeolite, leading to greater BTX formation and coke deposition. In contrast, the diffusion resistance of the light olefin products was low within the nano-sized zeolite, so such reaction was suppressed, leading to higher yield of light olefins as well as less coke formation. Clear differences were observed in the H/C atomic ratio of cokes deposited on nano- and macro-sized zeolites, and the ratio was smaller in the macro-sized zeolite than in the nano-sized zeolite. The H/C atomic ratio can be considered as an index of the aromaticity of the coke, in which the ratio is lower than 1 for poly-aromatics compounds and decreases with increased number of condensed aromatic rings[23]. Therefore, the aromaticity of the coke on the zeolites increased with greater amount of coke, and coke formed on macro-sized zeolite after the reaction consisted of poly-aromatic compounds. As a result, the nano-sized zeolite exhibited high and stable activity with low coke formation compared with the macro-sized zeolite, leading to the high yield of light olefins.

Finally, to examine regeneration of the zeolite catalyst, the nano-sized zeolite after reaction (18 h) was regenerated by calcination in air at 923 K for 3 h, and the regenerated zeolite was used as the catalyst for *n*-hexane cracking. The changes in *n*-hexane conversion and product selectivities over the regenerated zeolite are shown in **Figs. 9** and **10**, respectively. The regenerated zeolite exhibited almost the same *n*-hexane conversion and product selectivities as the fresh nano-sized zeolite. The ^{27}Al-NMR spectrum of the regenerated zeolite is also shown in **Fig. 4**. No peaks assigned to octahedrally coordinated aluminum were observed in the regenerated nano-zeolite. Accordingly, the nano-sized zeolite is an effective catalyst to produce light olefins from *n*-hexane.

3. Conclusion

MFI-type zeolites exhibited high cracking activity and provided high yields of light olefins. To identify the most effective catalyst for *n*-hexane cracking, the effect of the Si/Al ratio of the MFI-type zeolite on the catalytic activity and product yield was investigated. The Si/Al ratio affected *n*-hexane conversion, and the major light olefin component was propylene at low conversions. The maximum light olefin yield of approximately 35 C-mol% was obtained for a MFI-type zeolite with a Si/Al ratio of 150. Moreover, macro- and nano-sized zeolites with crystal sizes of approximately 1.5 μm and 150-200 nm, respectively, were prepared, and the effect of crystal size on the catalytic stability was investigated. The amount of coke deposited on the nano-sized zeolite was much smaller than that on the macro-sized zeolite. Accordingly, the nano-sized zeolite exhibited high and stable activity with low coke formation compared with the macro-sized zeolite.

Acknowledgment

This work was supported by a Research Grant Program from the New Energy and Industrial Technology Development Organization (NEDO) of Japan and the Global COE Program (Project No. B01: Catalysis as the Basis for Innovation in Materials Science from the Ministry of Education, Culture, Sports, Science and Technology, Japan).

References

1) Bortnovsky, O., Sazama, P., Wichterlova, B., *Appl. Catal. A: General*, **287**, 203 (2005).
2) Mei, C., Wen, P., Liu, Z., Wang, Y., Yang, W., Xie, Z., Hua, W., Gao, Z., *J. Catal.*, **258**, 243 (2008).
3) Jung, J. S., Park, J. W., Seo, G., *Appl. Catal. A: General*, **288**, 149 (2005).
4) Komatsu, T., Ishihara, H., Fukui, Y., Yashima, T., *Appl. Catal. A: General*, **214**, 103 (2001).
5) Plotkin, J. S., *Catal. Today*, **106**, 10 (2005).
6) Yoshimura, Y., Kijima, N., Hayakawa, T., Murata, K., Suzuki, K., Mizukami, F., Matano, K., Konishi, T., Oikawa, T., Saito, M., Shiojima, T., Shiozawa, K., Wakui, K., Sawada, G., Sato, K., Matsuo, S., Yamaoka, N., *Catal. Surv. Jpn.*, **4**, 157 (2000).
7) Magnoux, P., Cartraud, P., Mignard, S., Guisnet, M., *J. Catal.*, **106**, 242 (1987).
8) Corma, A., Gonzàlez-Alfaro, V., Orchillès, A. V., *Appl. Catal. A: General*, **129**, 203 (1995).
9) Katada, N., Kageyama, Y., Takahara, K., Kanai, T., Beguma, H. A., Niwa, M., *Catal. A Chem.*, **211**, 119 (2004).
10) Sugi, Y., Kubota, Y., Komura, K., Sugiyama, N., Hayashi, M., Kim, J. H., Seo, G., *Appl. Catal. A: General*, **299**, 157 (2006).
11) Inagaki, S., Kamino, K., Kikuchi, E., Matsukata, M., *Appl. Catal. A: General*, **318**, 22 (2007).
12) Tago, T., Iwakai, K., Morita, K., Tanaka, K., Masuda, T., *Catal. Today*, **105**, 612 (2005).
13) Tago, T., Konno, H., Sakamoto, M., Nakasaka, Y., Masuda, T., *Appl. Catal. A: General*, **403**, 183 (2011).
14) Tago, T., Nishi, M., Kouno, Y., Masuda, T., *Chem. Lett.*, **33**, 1040 (2004).
15) Tago, T., Iwakai, K., Nishi, M., Masuda, T., *J. Nanosci. Nanotechnol.*, **9**, 612 (2009).
16) Tago, T., Aoki, D., Iwakai, K., Masuda, T., *Top. Catal.*, **52**, 865 (2009).
17) Tago, T., Sakamoto, M., Iwakai, K., Nishihara, H., Mukai, S. R., Tanaka, T., Masuda, T., *J. Chem. Eng. Jpn.*, **42**, 162 (2009).
18) Iwakai, K., Tago, T., Konno, H., Nakasaka, Y., Masuda, T., *Micropor. Mesopor. Mater.*, **141**, 167 (2011).
19) Tago, T., Okubo, Y., Mukai, S. R., Tanaka, T., Masuda, T., *Appl. Catal. A: General*, **290**, 54 (2005).
20) Haag, W. O., Dessau, R. M., Proc. 8th Int. Congr. Catal.,

Berlin, vol. 2, 1984, p. 305.
21) Williams, B. A., Babitz, S. M., Miller, J. T., Snurr, R. Q., Kung, H. H., *Appl. Catal. A: General*, **177**, 161 (1999).
22) Williams, B. A., Ji, W., Miller, J. T., Snurr, R. Q., Kung, H. H., *Appl. Catal. A: General*, **203**, 179 (2000).
23) Guisnet, M., Magnoux, P., *Appl. Catal. A: General*, **212**, 83 (2001).

……

要　　旨

n-ヘキサン接触分解による低級オレフィン選択合成における MFI 型ゼオライトの結晶サイズと Si/Al 比の影響

今野　大輝，岡村　拓哉，中坂　佑太，多湖　輝興，増田　隆夫

北海道大学大学院工学研究院有機プロセス工学部門化学システム工学研究室，060-8628 札幌市北区北13条西8丁目

MFI 型ゼオライト触媒による *n*-ヘキサンの接触分解について検討した。ゼオライト触媒の酸点密度や結晶サイズについて詳細に検討するため，熱分解の影響がほとんどない反応温度 823 K で行った。MFI 型ゼオライトによる *n*-ヘキサン接触分解では，触媒活性が安定しており，酸点密度の異なる MFI 型ゼオライトを用いた場合，生成物収率と *n*-ヘキサン転化率の関係は一本の曲線で表せることが明らかになった。さらに，結晶サイズの異なるマクロクリスタル（1.5 μm）とナノクリスタル（150-200 nm）を合成し，ゼオライト触媒の結晶サイズが触媒活性や低級オレフィン収率に与える影響について検討した。ナノクリスタルを用いた場合，マクロクリスタルと比較して，低級オレフィン選択率が高く，高活性を維持する結果となった。これは，マクロクリスタルに析出したコーク量よりもナノクリスタルに析出したコーク量が少なかったことから，結晶サイズの微小化によって原料／生成物の細孔内拡散抵抗が低減したためであると考えられる。このように MFI 型ゼオライトナノクリスタルによる *n*-ヘキサンの接触分解は，長時間安定的に低級オレフィンを得られることが示唆された。

……